Available online at www.sciencedirect.com
ScienceDirect
Journal of Photochemistry and Photobiology A: Chemistry 189 (2007) 1–6
Journal of Photochemistry and Photobiology A:Chemistry
www.elsevier.com/locate/jphotochem

Nanophotocatalysis using nanoparticles of titania Mineralization and finite element modelling of Solophenyl dye decolorization

Niyaz Mohammad Mahmoodi [a,*], Nargess Yousefi Limaee [a], Mokhtar Arami [a,b], Shahin Borhany [b], Mahboobeh Mohammad-Taheri [a,b]

[a] *Colorant Manufacturing and Environmental Science Department, Institute for Colorants, Paint and Coating, Tehran, Iran*
[b] *Amirkabir University of Technology (Tehran Polytecnic), Tehran, Iran*

Received 26 August 2006; received in revised form 18 November 2006; accepted 16 December 2006
Available online 21 December 2006

Abstract

This paper investigates the mineralization and numerical finite element model for simulation of decolorization of Solophenyl Red 3BL (SR) by nanophotocatalysis using immobilized titania nanoparticle. A simple and effective method was developed for the immobilization of titania nanoparticles. UV–vis, ion chromatography (IC) and total organic carbon (TOC) analyses were employed to obtain the details of the photocatalytic decolorization and mineralization of SR. The nitrate and sulfate anions were detected as photocatalytic mineralization products of SR. Ninety-two percent total organic carbon can be eliminated after 240 min of irradiation time.The SEEP/W model was incorporated into the CTRN/W model and modified to solve mathematical equation describing decolorization process. The numerical model was first calibrated with an analytical equation for a simple mass transport problem through groundwater flow system. The simulation results were then compared to those results obtained from an experimental test for the decolorization of SR by nanophotocatalysis process and close agreement was achieved.

Keywords: Nanophotocatalysis; Finite element model; Immobilized titania nanoparticle; Mineralization; SEEP/W and CTRN/W models

1. Introduction

Many industries use synthetic dyes to color their products. The textile industry ranks first in the consumption of the dyes. Waste effluents discharging from such industries create serious problems to various segments of the environment. Dyes in waters affect the nature of the water, inhibiting light penetration into the streams and reducing the photosynthetic reaction. Some dyes are toxic and even at very low concentrations may seriously affect aquatic life. Some other dyes may cause allergy, skin irritation and cancer to humans [1–8].

Therefore, in order to minimise the risk of pollution problems from such effluents, it becomes crucial that dye be removed from effluents before discharging to the environment.

Considerable attempts have been done by many researchers to find appropriate treatment systems in order to treat effluents containing dyes. The most commonly used methods for dye removal from waste effluents are: physicochemical, chemical, and biological methods, such as adsorption techniques [6–8], electrochemical method [9], microbiological decomposition [10], and chemical coagulation [11]. Each method has its advantages and disadvantages. For example, although adsorption process using activated carbon in particular is economically cost method for dye removal, but high price, high operating costs, non-destructive nature, and problems with regeneration limit the applicability of this method for dye removal [12]. This process only transfers dyes from aqueous phase to solid phase, causing secondary pollution problem. For adsorption case, further treatment facilities are indeed required in order to separate the purified effluents or to regenerate the adsorbents. The electrochemical decomposition procedures are not efficient because many dyes cannot be easily decomposed [9]. Due to the large degree of aromatics present in many dye molecules and the

* Corresponding author. Tel.: +98 21 22956126; fax: +98 21 22947537.
E-mail address: nm_mahmoodi@yahoo.com (N.M. Mahmoodi).

1010-6030/$ – see front matter © 2006 Elsevier B.V. All rights reserved.
doi:10.1016/j.jphotochem.2006.12.025

Table 1
Properties of SR

Parameter	SR
C.I. number	35780
Commercial name	Solophenyl Red 3BL
Empirical formula	$C_{25}H_{26}N_{10}O_{21}S_6Na_6$
Formula weight (g/mol)	1132

stability of modern dyes, the biological treatment methods are ineffective for degradation process. Filtration potentially provides pure water, but low molar mass dyes can pass through the filter system. Coagulation using alums, ferric salts, or limes is a low cost process. On the other hand, it requires extra costs for disposal of the waste. Therefore, there is a growing interest to design appropriate treatment systems that lead to the complete destruction of the dye molecules. Nanophotocatalysis using nanostructuring of materials such as TiO_2 nanoparticle constitutes one of the emerging technologies for the degradation of organic pollutants. Several advantages of this process over competing processes are: complete mineralization, no waste-solids disposal problem, and only mild temperature and pressure conditions are necessary [1–5,13,14].

Photocatalytic degradation of organic pollutants, such as dyes and pesticides is well-established process in our laboratory [1–5,15,16], but little researches have been carried out to modelling the photocatalytic degradation of dyes in literature. There are more recent papers involving numerical finite element model on the other area [17–20]. The main objective of this paper is to investigate the mineralization and numerically model the photocatalytic decolorization of SR using nanophotocatalysis. The numerical simulation considers a first-order model for the photocatalytic decolorization rate. A user-friendly commercial package called SEEP/W was integrated into the CTRN/W [21] model, incorporating the numerical finite element approach, and slightly modified to simulate the photocatalytic degradation process.

2. Experimental

2.1. Reagents

Solophenyl Red 3BL was obtained from Ciba. The descriptions (name, color, and molecular weight) of SR and its chemical structure are shown in Table 1 and Fig. 1. Titania nanoparticle (Degussaa P25) was utilized as a photocatalyst. Its main physical data are as follows: average primary particle size 30 nm, purity above 97%, and with 80:20 anatase to rutile. Other chemicals were purchased from Merck.

Fig. 1. The chemical structure of SR.

2.2. Developed method for immobilization of titania nanoparticles

A simple and effective method was developed for the immobilization of TiO_2 nanoparticles as follows: inner surfaces of reactor walls were cleaned with acetone and distilled water to remove any organic or inorganic material attached to or adsorbed on the surface and was dried in the air. A pre-measured mass of TiO_2 nanoparticle (16 g) was attached on the inner surfaces of reactor walls using a thin layer of a UV resistant polymer. Immediately after preparation, the inner surface reactor wall–polymer–TiO_2 nanoparticle system was placed in the laboratory for at least 60 h for complete drying of the polymer [1–5,15,16].

2.3. Photocatalytic reactor

Experiments were carried out in a batch mode immersion rectangular immobilized TiO_2 nanoparticle photocatalytic reactor made of Pyrex glass. Two UV-C lamps (15 W, Philips) were used as the radiation source. An air pump was utilized for the mixing and aeration of dye solution. The total volume of reactor is 17 L.

2.4. Analyses

Photocatalytic decolorization and mineralization processes were performed using a 6 L solution containing specified concentration of dye. Solutions were prepared using distilled water to minimize interferences. The initial concentration of SR was 0.044 mM. The photocatalytic degradation processes were carried out at 298 K. Samples were withdrawn from sample point at certain time intervals and analyzed for decolorization and mineralization.

Decolorization of dye solution was checked and controlled by measuring the maximum absorbance at 543 nm (λ_{max}) of dye solutions at different time intervals by UV–vis CECIL 2021 spectrophotometer.

Ion chromatograph (METROHM 761 Compact IC) was used to assay the appearance and quantity of formate, acetate, oxalate, SO_4^{2-} and NO_3^- ions formed during the decolorization and mineralization of SR using a METROSEP anion dual 2, flow 0.8 mL/min, 2 mM $NaHCO_3$/1.3 mM Na_2CO_3 as eluent, temperature 20 °C, pressure 3.4 MPa, and conductivity detector.

The TOC of the reaction solution was measured with a TOC-4000 Shimadzu analyzer.

3. Results and discussions

3.1. Mineralization of SR

SR is a tetrakis azo dye, which has a strong absorbance in the UV–visible region. The chromophore part containing azo linkage has an absorption in the visible region while benzene and naphthalene rings in the UV region, naphthalene ring absorption wavelength is higher than that of benzene ring. Hydrogen peroxide concentration is a key parameter on the photocatalytic

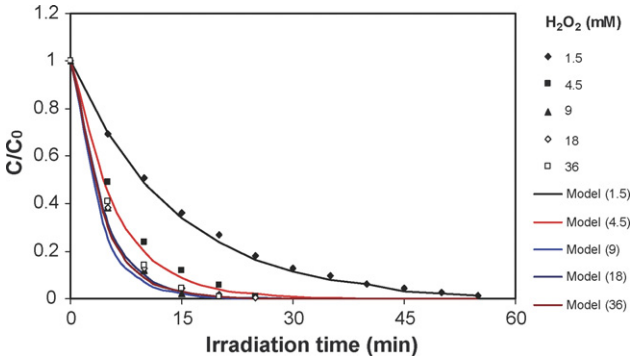

Fig. 2. Effect of hydrogen peroxide concentration on the decolorization of SR (dots) and comparison of SR decolorization rate predicted by finite element model (solid lines) and determined at laboratory (dots).

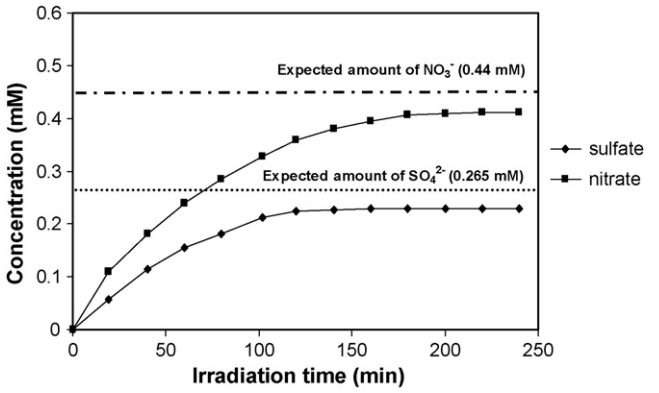

Fig. 4. Evolution of sulfate and nitrate ions during the photocatalytic mineralization of SR (dye: 0.044 mM, H_2O_2: 4.5 mM).

dye decomposition, depending on its concentration and nature of reductants. As seen in Fig. 2, the decolorization rate increased when H_2O_2 concentration changed from 0 to 4.5 mM. No appreciable changes were observed at decolorization time when the concentration further increased to 36 mM. A concentration of 4.5 mM appears to be optimal.

During the photocatalytic decolorization and mineralization of dye, various organic intermediates were produced. Consequently, destruction of the dye should be evaluated as an overall degradation process, involving the degradation of both the parent dye and its intermediates.

Further hydroxylation of aromatic intermediates leads to the cleavage of the aromatic ring resulting in the formation of oxygen-containing aliphatic compounds [1]. Formate, acetate, and oxalate were detected as important aliphatic carboxylic acid intermediates during the degradation of SR (Fig. 3). The formation of oxalate initially increased with the irradiation time, and then sharply dropped. After 240 min of irradiation, Carboxylic acids (formate, acetate, and oxalate) disappeared, indicating the mineralization of SR into CO_2.

Also, the photocatalytic mineralization of SR implies the appearance of inorganic products, mainly anions, since heteroatoms are generally converted into anions in which they are at their highest oxidation degree. The removal of total organic carbon (TOC) is commonly employed to indicate the mineralization of organic pollutants. To quantitatively characterize the mineralization of SR in the solution, the removal ratio was used in this study. The TOC removal ratio is about 92% after 240 min of irradiation. The overall stoichiometry for mineralization of SR can be written as:

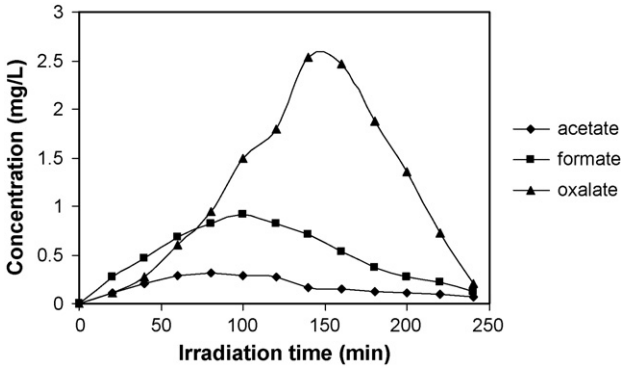

Fig. 3. Formation and disappearance of aliphatic carboxylic acids in the solution during the photocatalytic degradation of SR (dye: 0.044 mM, H_2O_2: 4.5 mM).

$$C_{25}H_{26}N_{10}O_{21}S_6Na_6 + 88H_2O_2 \rightarrow 25CO_2 + 10NO_3^- + 6SO_4^{2-} + 93H_2O + 16H^+ + 6Na^+ \quad (1)$$

Mineralization of SR is reported for an irradiation period of 240 min. The formation of SO_4^{2-} and NO_3^- from SR mineralization was shown in Fig. 4. It can be seen from Fig. 4 that the amount of SO_4^{2-} and NO_3^- anions increased and gradually reached to a maximum as the irradiation time increasing, indicating that the selected dye was mineralized. However, the quantity of sulfate ions released (0.23 mM) is lower than that expected from stoichiometry (0.265 mM). This could be first explained by a loss of sulfur-containing volatile compounds, such as H_2S and/or SO_2. However, this is not probable since both gases are very soluble in water and known as readily oxidizable into sulfate by nanophotocatalysis. The more probable explanation for the quantity of SO_4^{2-} obtained smaller than that expected from stoichiometry is given by the partially irreversible adsorption of some SO_4^{2-} ions at the surface of titania as already observed. However, this partial adsorption of SO_4^{2-} ions does not inhibit the photocatalytic degradation of pollutants [1,14]. Also, the quantity of nitrate ions released (0.41 mM) is lower than that expected from stoichiometry (0.44 mM) indicating that N-containing species remain adsorbed in the photocatalyst surface or most probably, that significant quantities of N_2 and/or NH_3 have been produced and transferred to the gas-phase. In azo bond each nitrogen atom is in its +1 oxidation degree. This oxidation degree favors the evolution of gaseous dinitrogen by the two step reduction process expressed previously. N_2 evolution constitutes the ideal case for a decontamination reaction involving totally innocuous nitrogen-containing final product [14].

3.2. Numerical modelling of SR decolorization

In this paper, a numerical model incorporating the finite element descretization scheme is presented to simulate the

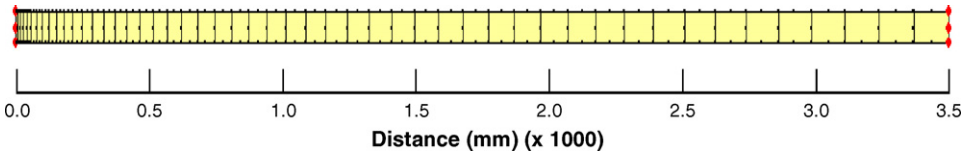

Fig. 5. Finite element representation of the solute transport model.

photocatalytic decolorization of SR using nanophotocatalysis process.

3.2.1. Modelling governing equation

The partial differential equation describing the photocatalytic decolorization process is given by Eq. (2). This equation was numerically solved using CTRN/W model in order to simulate the dye removal from aqueous solution. It was assumed that the photocatalytic decolorization is the only mechanism for dye removal in a batch system.

$$\frac{\partial C}{\partial t} = -kC \tag{2}$$

where C is the dye concentration in aqueous system (mM), k the first-order rate constant (s^{-1}), t the time (s), and x is the cartesian coordinates (mm).

3.2.2. Modelling tool

A commercial numerical finite element package called CTRN/W was coupled with SEEP/W, another model that creates the finite element grid [21] and slightly modified to simulate the photocatalytic decolorization of SR from aqueous solution. The main processes incorporated in CTRN/W are diffusion, dispersion, adsorption, radioactive decay, and density dependencies. CTRN/W model utilises the SEEP/W finite element grid to model photo-degradation process. In all CTRN/W simulation, the following partial differential equation is solved:

$$\left(\theta + \rho_d \frac{\partial S}{\partial C}\right) \frac{\partial C}{\partial t} = \theta D \frac{\partial^2 C}{\partial x_j^2} - U_j \frac{\partial C}{\partial x_j} - kS\rho_d - k\theta C \tag{3}$$

where θ is the volumetric water content (dimensionless), C the concentration (mM), D the hydrodynamic dispersion coefficient (mm^2/s), x_j the cartesian coordinates (mm), U_j the Darcian velocity in the x_j direction (mm/s), ρ_d the bulk density of the medium (1/1000 mg/ml), S the concentration in the solid phase (mg/g), t the time (s), and k is the first-order rate constant (s^{-1}).The first-order kinetic constant k can be related to the half-time T(s) for decaying substance as follows:

$$T = \frac{0.693}{k} \tag{4}$$

This modification is necessary to be considered when the CTRN/W model is used for simulation purpose.

3.2.3. Model validation

The finite element model was first checked by comparison with an analytical solution for a one-dimensional advection–dispersion contaminant transport equation under steady state water flow condition. In this case, the volumetric water content was 0.5. The dispersivity (α_L) was 150 mm and the molecular diffusion coefficient (D_{dif}) was negligible. The Darcian velocity (U) was equal to 0.15 mm/s. The hydrodynamic dispersion coefficient was calculated as:

$$D = D_{dif} + \alpha_L \times \frac{U}{\theta} = 0 + 150 \times \frac{0.15}{0.5} = 45\ mm^2/s \tag{5}$$

The following equation [22] was first used to solve the problem analytically.

$$C = \frac{C_0}{2}\left\{\text{erfc}\left(\frac{x - Vt}{2\sqrt{Dt}}\right) + \exp\left(\frac{Vx}{D}\right)\text{erfc}\left(\frac{x + Vt}{2\sqrt{Dt}}\right)\right\} \tag{6}$$

where C_0 is the source concentration of pollutant, V the average linear velocity, and erfc is the complement of the error function.

To solve the problem numerically, a 3500 mm horizontal profile was divided into 50 non-uniform quadratic elements using SEEP/W model. The model contained 253 nodes and 60 mm thickness (Fig. 5).

A constant head of 100 m was assigned at the inlet boundary of the model. A constant head of 90 m was also maintained at the outer boundary. The permeability was considered 5.2542×10 mm/s. These settings produced a constant Darcian velocity equal to 0.15 mm/s. The volumetric water content was set to 0.5. A simulation was then performed at a steady state condition.

In order to perform the main part of the mass transport simulation by the CTRN/W software, the finite element model constructed by the SEEP/W software was first imported into CTRN/W model. A first-type or Dirichlet boundary condition was considered at inlet ($x = 0$), with $C(0, t) = 1$ mM.

An initial value of 0 was maintained at $t = 0$. A value of 0 was specified at outlet boundary ($C(\infty, t) = 0$). Fifty time steps were considered. A total iteration of 20 was assigned for the

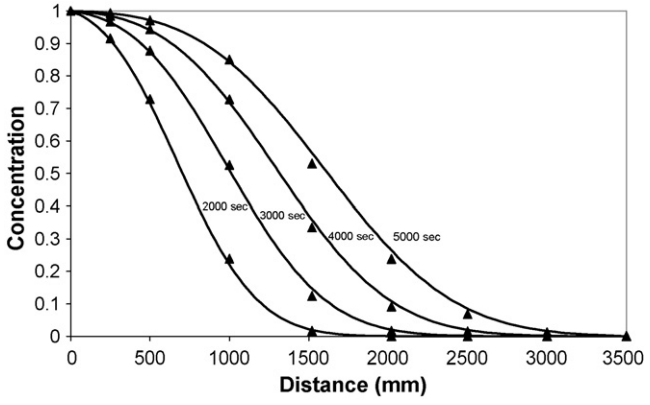

Fig. 6. Comparison of analytical (▲) and numerical (—) solutions for mass transport problem through groundwater system.

Table 2
Model input data used for the simulation of photocatalytic decolorization of SR

Input parameter	Value
Dye initial concentration (mM)	0.044
Kinetic constant (1/min)	Table 3
Number of iterations	50
Number of time steps	13
Time integration scheme	Central difference

simulation. A central difference time integration scheme was selected. The longitudinal dispersivity was set to 50 mm.

The comparison of the relative concentrations predicted by the finite element model (line) and those calculated using Eq. (6) (triangles) are shown in Fig. 6. The agreements between two methods are quite close. As the figure shows, the results were given for different elapsed times of 2000, 3000, 4000, and 5000 s.

3.2.4. Model prediction

In order to model the photocatalytic decolorization of SR from the solution phase, a one-dimensional simulation was performed using CTRN/W package. The model input data are given in Table 2. Table 3 shows the first-order rate constants for SR.

In first stage of the simulation using SEEP/W software, a one-dimensional finite element model incorporating 50 equal size elements and 253 nodes and with a length of 380 mm was constructed. The x-direction of cartesian coordinate was used to simulate horizontal batch system in which photocatalytic decolorization takes place. The hydraulic head differential and hydraulic conductivity were selected to produce zero velocity in order to neglect the advection term in Eq. (3). The volumetric water content θ was defined as a constant equal to 1. A steady state simulation was then performed.

The associated SEEP/W model was included with the CTRN/W software. To specify the input data, the material properties box was selected from the KeyIn menu. The longitudinal and transverse dispersivities were set to 1×10^{-20} mm. The kinetic constant (or decay half-life) was considered to be zero. A value equal to the initial dye concentration in the solution system (0.044 mM) was specified at all nodal points of the finite element grid. A small time step of seconds was assigned to consider the simulation as a steady state condition. The SOLVE window was then 1×10^{-20} mm used to perform this steady state simulation and provide the initial conditions for the main transient modelling of the photocatalytic decolorization process (third step).

Table 3
First-order rate constants for photocatalytic decolorization of SR

H_2O_2 (mM)	k (1/min)	R^2
1.5	0.07	0.99
4.5	0.17	0.94
9.0	0.21	0.97
18	0.21	0.99
36	0.22	0.98

To perform the third stage of the simulation, the dye initial concentration was first removed from all nodal points. A total iteration of 50 was assigned for the simulation. A central difference time integration scheme was considered. For transient modelling, 13 time steps were assigned. The model was then run for a simulation time of 60 min.

Fig. 2 compares experimental data and model predictions for the relative concentrations of SR as a function of irradiation time. The agreement between the predicted results and measured data are somewhat close. This figure was plotted for different H_2O_2 concentrations.

4. Conclusion

This paper examines the mineralization and numerical model for simulation of decolorization of Solophenyl Red 3BL by nanophotocatalysis using immobilized titania (TiO_2) nanoparticle. The governing equation describing the photocatalytic degradation of dyes was numerically solved using the finite element descretization scheme. As simulation tool, a student version of SEEP/W model was integrated into CTRN/W model and slightly modified to solve mathematical equation describing decolorization process. Both experimental and modelling process showed that the SR was successfully decolorized and degraded by this chemical process. First-order model describes well the photocatalytic decolorization kinetics. The results obtained from this investigation can help to design an appropriate wastewater management strategy based on the photocatalytic degradation to minimise the socio-economic and environmental impacts of textile effluents.

References

[1] N.M. Mahmoodi, M. Arami, J. Photochem. Photobiol. A: Chem. 182 (2006) 60–66.
[2] N.M. Mahmoodi, M. Arami, N.Y. Limaee, N.S. Tabrizi, J. Colloid Interface Sci. 295 (1) (2006) 159–164.
[3] N.M. Mahmoodi, M. Arami, N.Y. Limaee, J. Hazard. Mater. B 133 (1–3) (2006) 113–118.
[4] N.M. Mahmoodi, M. Arami, N.Y. Limaee, K. Gharanjig, F.D. Ardejani, Colloid Surf. A: Physicochem. Eng. Aspects 290 (2006) 125–131.
[5] N.M. Mahmoodi, M. Arami, N.Y. Limaee, N.S. Tabrizi, Chem. Eng. J. 112 (1–3) (2005) 191–196.
[6] M. Arami, N.Y. Limaee, N.M. Mahmoodi, N.S. Tabrizi, J. Colloid Interface Sci. 288 (2) (2005) 371–376.
[7] M. Arami, N.Y. Limaee, N.M. Mahmoodi, N.S. Tabrizi, J. Hazard. Mater. B 135 (2006) 171–179.
[8] M. Arami, N.Y. Limaee, N.M. Mahmoodi, Chemosphere 65 (2006) 1999–2008.
[9] A.G. Vlyssides, M. Loizidou, P.K. Karlis, A.A. Zorpas, D. Papaioannou, J. Hazard. Mater. 70 (1999) 41–52.
[10] C.L. Pearce, J.R. Lloyd, J.T. Guthrie, Dyes Pigments 58 (2003) 179–196.
[11] S. Venkata Mohan, P. Sailaja, M. Srimurali, J. Karthikeyan, Environ. Eng. Policy 1 (1999) 149–154.
[12] Z. Aksu, Process Biochem. 40 (2005) 997–1026.
[13] M.R. Hoffmann, S.T. Martin, W. Choi, D.W. Bahneman, Chem. Rev. 95 (1995) 69–96.
[14] I.K. Konstantinou, T.A. Albanis, Appl. Catal. B: Environ. 49 (2004) 1–14.
[15] N.M. Mahmoodi, M. Arami, N.Y. Limaee, K. Gharanjig, F. Nourmohammadian, Mater. Res. Bull. 42 (2007) 797–806.

[16] N.M. Mahmoodi, M. Arami, N.Y. Limaee, K. Gharanjig, J. Hazard. Mater. (2006), doi:10.1016/j.jhazmat.2006.10.089.
[17] D. Garriga-Majo, R.J. Paterson, R.V. Curtis, R. Said, R.D. Wood, J. Bonet. Dent. Mater. 20 (5) (2004) 409.
[18] J. Mackerle, Comput. Methods Biomech. Biomed. Engin. 8 (2) (2005) 59–81.
[19] J. Mackerle, Comput. Methods Biomech. Biomed. Engin. 7 (5) (2004) 277–303.
[20] J.S. Raul, D. Baumgartner, R. Willinger, B. Ludes, Int. J. Legal Med. 120 (4) (2006) 212–218.
[21] Geo-slope International Ltd., SEEP/W and CTRN/W for Finite Element Seepage and Mass Transport Analyses. Geo-slope, 2002, http://www.geo-slope.com/products/seepw.asp.
[22] L.N. Reddi, H.I. Inyang, Geoenvironmental Engineering, Principles and Applications, Marcel Dekker, Inc., New York, 2000, p. 494.